Identification of Conformationally Sensitive Amino Acids in the Na^+/Dicarboxylate Symporter (SdcS)[†]

Aditya D. Joshi[‡] and Ana M. Pajor*[,§,||]

Department of Molecular Physiology and Biophysics, Baylor College of Medicine, Houston, Texas 77030, and Skaggs School of Pharmacy and Pharmaceutical Sciences, University of California—San Diego, La Jolla, California 92093-0718

Received December 11, 2008; Revised Manuscript Received February 26, 2009

ABSTRACT: The Na^+/dicarboxylate symporter (SdcS) from S*taphylococcus aureus* is a homologue of the mammalian Na^+/dicarboxylate cotransporters (NaDC1) from the solute carrier 13 (SLC13) family. This study examined succinate transport by SdcS heterologously expressed in *Escherichia coli*, using right-side-out (RSO) and inside-out (ISO) membrane vesicles. The K_m values for succinate in RSO and ISO vesicles were similar, ~30 μM. The single cysteine of SdcS was replaced to produce the cysteine-less transporter, C457S, which demonstrated functional characteristics similar to those of the wild type. Single-cysteine mutants were made in SdcS-C457S at positions that are functionally important in mammalian NaDC1. Mutant N108C of SdcS was sensitive to chemical labeling by MTSET {[2-(trimethylammonium)-ethyl]methanethiosulfonate} from both the cytoplasmic and extracellular sides, depending on the conformational state of the transporter, suggesting that Asn-108 may be found in the translocation pore of the protein. Mutant D329C was sensitive to MTSET in the presence of Na^+ but only from the extracellular side. Finally, mutant L436C was insensitive to MTSET, although changes in its kinetic properties indicate that this residue may be important in substrate binding. In conclusion, this work identifies Asn-108 as a key residue in the translocation pathway of the protein, accessible in different states from both sides of the membrane. Functional characterization of SdcS should provide useful structural as well as functional details about mammalian transporters from the SLC13 family.

The Na^+/dicarboxylate symporter (SdcS) from *Staphylococcus aureus* is a member of the divalent anion sodium symporter (DASS) family that also includes the mammalian solute carrier 13 (SLC13)[1] family (*1*). SLC13 family members are plasma membrane transporters that use energy from the movement of Na^+ down its electrochemical gradient to transport dicarboxylates or inorganic anions across the membrane (*2*). There are three different SLC13 transporters for citric acid cycle intermediates in humans: the low-affinity Na^+/dicarboxylate cotransporter 1 (NaDC1), the high-affinity Na^+/dicarboxylate cotransporter 3 (NaDC3), and the Na^+/citrate cotransporter (NaCT). The transport properties of SdcS are very similar to those of the mammalian NaDC transporters. SdcS is a Na^+-coupled transporter that carries four-carbon terminal dicarboxylates, including succinate, malate, and fumarate, with K_m values between 5 and 15 μM (*3*).

Although a considerable amount of structure—function information has been gained using the mammalian NaDC transporters (*4*—*7*), there are technical difficulties with mammalian expression systems that limit the studies to the extracellular surface of the membrane. In contrast, prokaryotic homologues of mammalian proteins can be expressed in large quantities in bacteria such as *Escherichia coli*, which allows detailed structural and functional characterization (*8, 9*). Established methods for preparing *E. coli* membrane vesicles of known orientation permits the analysis of transporters from both the inside and outside of the cell (*10*—*12*). The sequence of SdcS is ~35—40% identical to that of the mammalian NaDC1 transporters, and several key residues are conserved or are similar. Therefore, studies of SdcS should provide valuable information that is applicable to the other members of the DASS family.

In this study, we examined the functional properties of SdcS and mutants expressed in *E. coli*, using right-side-out (RSO) and inside-out (ISO) membrane vesicles to examine the transport reactions in both directions. SdcS exhibited similar succinate K_m values in RSO compared with ISO vesicles. The cysteine-less transporter C457S had kinetic properties similar to those of the wild type, although there were some differences in the effects of sodium on transport. We also found that amino acids previously found to be important in mammalian NaDC1 are also important in SdcS. The N108C mutant of SdcS was found to be accessible to

[†] This work was supported by National Institutes of Health Grant DK46269 (A.M.P.).

* To whom correspondence should be addressed: Skaggs School of Pharmacy and Pharmaceutical Sciences, University of California—San Diego, La Jolla, CA 92093-0718. Telephone: (858) 822-7806. Fax: (858) 822-5591. E-mail: apajor@ucsd.edu.

[‡] Baylor College of Medicine.

[§] University of California—San Diego.

[||] Portions of this work were conducted at the Department of Biochemistry and Molecular Biology, University of Texas Medical Branch, Galveston, TX 77555.

[1] Abbreviations: IPTG, isopropyl β-D-galactopyranoside; ISO, inside-out; KP_i, potassium phosphate buffer; MTSET, [2-(trimethylammonium)ethyl]methanethiosulfonate; NaDC1, sodium dicarboxylate cotransporter 1; PMSF, phenylmethanesulfonyl fluoride; rb, rabbit; RSO, right-side-out; SLC13, solute carrier 13; TM, transmembrane helix.

10.1021/bi8022625 CCC: $40.75
Published on Web 03/04/2009

membrane impermeant methanethiosulfonate reagents from both sides of the membrane, indicating that this residue may be located within the translocation pathway of the transporter, possibly close to the substrate binding site. The D329C mutant was accessible to MTSET in RSO vesicles and only in the conformation seen in the presence of Na^+. Mutant L436C was not functionally affected by MTSET treatment, but this mutant exhibited a decrease in substrate affinity in the forward direction. In conclusion, this study establishes SdcS as a model system for the eukaryotic NaDC1 transporters and identifies key residues that may be important during the transport cycle from both sides of the membrane.

EXPERIMENTAL PROCEDURES

Site-Directed Mutagenesis. Site-directed mutagenesis was performed using the QuikChange site-directed mutagenesis kit (Stratagene) according to the manufacturer's instructions. Plasmid pQE-80L/SdcS encoding SdcS with a hexahistidine tag at the N-terminus (*3*) was used as a template to construct the cysteine-less mutant, C457S. The cysteine-substituted mutants were then made using the C457S mutant as a template. Mutants were verified by sequencing at the University of Texas Medical Branch (Galveston, TX) DNA Sequencing facility.

Preparation of Membrane Vesicles. Expression of recombinant SdcS in *E. coli* BL21 [F^- ompT $hsdS_B(r_B^- m_B^-)$ gal dcm] was as described previously (*3*). Overnight cultures of *E. coli* transformed with plasmids (SdcS and mutants C457S, D329C, L436C, and N108C in vector pQE-80L or pQE-80L alone) were used to inoculate 500 mL of LB-Lennox broth (1:10 dilution) containing 50 μg/mL carbenecillin. Cells were grown at 37 °C to an optical density at 660 nm of 0.4−0.6. To induce protein expression, 150 μM isopropyl β-D-galactopyranoside (IPTG) was added and cells were harvested 2 h later by centrifugation. Cell pellets were washed and resuspended with 100 mM potassium phosphate (KP_i) buffer (pH 7).

Right-side-out (RSO) vesicles were prepared by a modification of Kaback's method developed by Quick and Jung (ref *12* and personal communication from M. Quick). Briefly, washed centrifuged cell pellets were resuspended in 300 mL per liter of original culture of 30% sucrose and 30 mM Tris-HCl (pH 8). RNase A (1 μg/mL) and K_2-EDTA (pH 7, 10 mM) were added, and the mixture was incubated at room temperature for 2−3 min. Lysozyme (6.4 mg to 300 mL of resuspended pellets) was added, and flasks were incubated with shaking for 15 min at room temperature. The cell suspension was centrifuged for 30 min at 17000*g* (r_{av}), and pellets were resuspended in 7.5 mL of 30% sucrose, 20 mM $MgSO_4$, 100 mM potassium phosphate (KP_i) buffer (pH 6.6). RNase A and DNase (1.7 mg each) were added, and homogenates were poured into 1 L flasks containing 600 mL of 50 mM KP_i (pH 6.6). Flasks were incubated for 10 min at 30 °C with slow shaking at 75 rpm. K_2-EDTA (1 M, pH 7; final concentration of 10 mM) was added and the incubation continued for 15 min, followed by 1 M $MgSO_4$ (final concentration of 15 mM) and an additional 15 min incubation. The cells were centrifuged at 27500*g* for 70 min. The pellets were resuspended in a total volume of approximately 100 mL of 100 mM KP_i and 10 mM EDTA (pH 6.6). Low-speed centrifugation was performed at ~500*g* for 30 min to remove unbroken cells. The supernatants were then centrifuged at 43400*g* for 30 min. RSO vesicles were resuspended by homogenization in 100 mM KP_i (pH 7), separated into aliquots, quick-frozen in liquid N_2, and stored at −80 °C.

Inside-out membrane vesicles (ISO) were prepared according to the method of Quick and Jung (refs *12* and *13* and personal communication from M. Quick), with an additional step to purify the membranes by sucrose density gradient centrifugation (*14*). The cells were washed and suspended in KP_i buffer (pH 7.4) to approximately 50 mL per liter of culture. Phenylmethanesulfonyl fluoride (PMSF, 0.5 mM) was added to all steps to reduce proteolysis. The suspensions were incubated on a platform shaker at 4 °C with 0.5 mg/mL DNase and 0.5 mg/mL RNase A. The cell suspensions were then passed through a French pressure cell (Thermo Scientific) at 4000 psi. Unbroken cells and organelles were removed by low-speed centrifugation for 15 min at 10000*g* and 4 °C. Vesicles were then pelleted from the supernatants by ultracentrifugation at ~184000*g* for 45 min at 4 °C. The pellets were resuspended by homogenization in 2 mL of 100 mM KP_i buffer (pH 7.4) and further purified by sucrose density gradient centrifugation. The sucrose density step gradients were prepared with 0.77, 1.44, and 2.02 M sucrose in 10 mM HEPES (pH 7.4). Crude ISO vesicles were added to the top of the gradient, and samples were centrifuged at 27000 rpm (SW28 rotor, Beckman) for 15−18 h at 4 °C. The upper band of proteins at the interface between 0.77 and 1.44 M sucrose was collected with a gradient collector. Preliminary studies showed that this membrane fraction contains most of the Na^+-dependent succinate transport activity in vesicles prepared from *E. coli* expressing SdcS. The lower band between 1.44 and 2.02 M sucrose contains cell wall fragments and other cellular debris (*14*). The upper band from the step gradient containing ISO vesicles was diluted approximately 5-fold with 100 mM KP_i (pH 7.4) and centrifuged at ~184000*g* for 45 min at 4 °C. ISO membrane vesicles were resuspended by homogenization in 100 mM KP_i (pH 7.4). The vesicles were separated into aliquots, quick-frozen in liquid N_2, and stored at −80 °C. For each experiment, at least three independent right-side-out and inside-out membrane vesicle preparations were made.

Transport Assays. Uptake of [^{14}C]succinate by RSO and ISO membrane vesicles was measured using a rapid filtration assay (*15*). The sodium transport buffer contained (unless otherwise specified) 10 mM NaCl, 90 mM choline chloride, and 50 mM MOPS (pH adjusted to 7 with 1 M Tris). The assays were conducted at room temperature. For the assay, 40 μL of transport buffer containing ~30 μM [^{14}C]succinate (44 mCi/mmol, PerkinElmer Life Sciences) was placed in the bottom of a 5 mL polystyrene Falcon tube. The reaction was initiated by the addition of 10 μL of vesicles with vortexing. The reaction was terminated after the appropriate time, usually 10 s, with 1 mL of ice-cold choline buffer [100 mM choline chloride and 50 mM MOPS (pH 7)], filtered immediately through a Millipore filter (0.45 μm pore size, type HAWP) with suction, and washed with 4 mL of cold choline buffer. The radioactivity retained by the filters was measured by liquid scintillation counting.

Sodium activation of succinate uptake was determined by replacing Na^+ with choline up to a final concentration in the transport mixture of 80 mM. For experiments to

determine kinetic constants, succinate concentrations between 1 and 200 μM (or 400 μM for RSO vesicles containing the L436C mutant) were used. Kinetic constants (K_m and V_{max}) were determined by fitting initial transport rates (10 s) to the Michaelis−Menten equation [$v = (V_{max}[S])/(K_m + [S])$] using nonlinear regression analysis (SigmaPlot 9, Systat Software Inc.).

MTS Labeling. The MTSET labeling reaction was done by combining 40 μL of the vesicles with 10 μL of 5× concentrated solutions: 5 mM MTSET in either 25 mM Na^+/75 mM choline buffer, 100 mM choline buffer, or 25 mM Na^+/75 mM choline buffer with 50 mM succinate for 10 min at room temperature. MTSET was weighed into tubes, kept dark and on ice, and the buffer added just before use. A final MTSET concentration of 1 mM was used for all the preincubations. Control groups of vesicles were preincubated with the same buffers but without MTSET. After the preincubations, the transport activity remaining in the vesicles was measured as described above.

Immunoblot Analysis. RSO and ISO vesicles (25 μg of protein) were diluted in sample buffer [50 mM Tris-HCl (pH 7), 10% glycerol, 4% SDS, 2% β-mercaptoethanol, and 0.1 mg/mL Coomassie blue R-250] and heated in a boiling water bath for 2 min. Proteins were separated by Tricine SDS−PAGE with 10% (w/v) acrylamide and transferred to nitrocellulose membranes (*16*). Blots were incubated with 1:2000 dilutions of mouse monoclonal antibody reactive to the SdcS N-terminal $RGS(H)_4$ epitope tag (RGS-His antibody, QIAGEN) followed by 1:5000 dilution of the horseradish peroxidase-conjugated anti-mouse immunoglobulin G antibody (Jackson ImmunoResearch Laboratories, Inc.). The Supersignal West Pico chemiluminescent substrate kit (Pierce) was used to detect antibody binding. Images were captured with a Kodak Image Station 440CF, and Image 1D analysis software (Eastman Kodak Co.) was used to quantitate the protein expression.

Protein Determination. The protein content of membrane vesicles was measured using the Bio-Rad protein assay with γ-globulin as a standard.

Statistics. Duplicate or triplicate measurements were made for each data point. The experiments were repeated with at least three different membrane preparations. Significant differences between groups were identified by a Student's t test or ANOVA with $P < 0.05$.

RESULTS

Time Course of Na^+-Dependent Succinate Transport. Figure 1 shows time courses of succinate transport by right-side-out (RSO) and inside-out (ISO) membrane vesicles of *E. coli* BL21 cells harboring pQE-80L vector only, pQE-80L/SdcS, or pQE-80L/C457S, encoding the cysteine-less mutant. Vesicles expressing SdcS and C457S showed rapid accumulation of succinate followed by a slow decline. The succinate uptake was linear until ~15 s, and therefore, 10 s was used as an initial time point in subsequent experiments. The peak of the overshoot was seen at ~1 min for both SdcS and C457S in RSO and ISO vesicles. The succinate content of ISO vesicles expressing SdcS and C457S reached equilibrium by 60 min, whereas the RSO vesicles still retained some of their succinate content by that time point, possibly due to differences in membrane permeability or vesicle volume. The succinate content of vesicles prepared from *E. coli* carrying the control plasmid, pQE-80L, showed a steady increase toward equilibrium with no overshoot in succinate concentration. The time course of succinate transport by SdcS in choline was similar to that of vesicles containing the control plasmid (not shown).

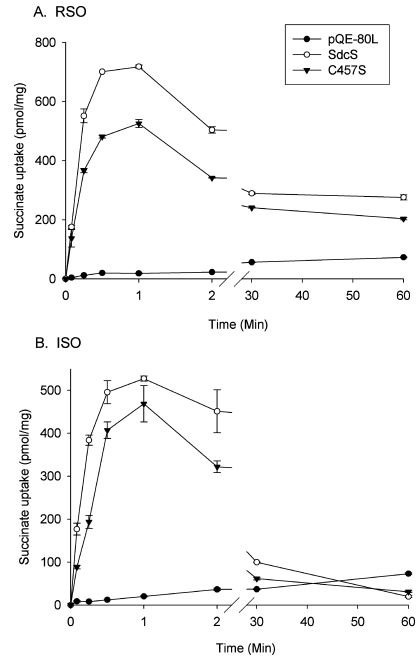

FIGURE 1: Time course of succinate uptake by right-side-out (RSO) and inside-out (ISO) membrane vesicles. Uptake of 30 μM [^{14}C]succinate was measured in transport buffer containing 10 mM Na^+ by (A) RSO and (B) ISO membrane vesicles of *E. coli* (BL21 strain) expressing SdcS or the cysteine-less mutant, C457S. Control vesicles were prepared from *E. coli* transformed with the pQE-80L plasmid. Results are presented as means ± the range of duplicate measurements from a single vesicle preparation. The experiment was repeated with similar results with three separate vesicle preparations.

Vesicle Orientation. To verify the orientation of RSO and ISO membrane vesicles, succinate transport activity was measured after pretreatment with membrane-impermeant cysteine-specific methanethiosulfonate (MTS) reagents. RSO and ISO membrane vesicles were preincubated for 10 min with 1 mM [2-(trimethylammonium)ethyl]methanethiosulfonate (MTSET) or 1 mM (2-sulfonatoethyl)methanethiosulfonate (MTSES). There was no effect of the MTS reagents on succinate uptake activity in RSO vesicles expressing SdcS (Figure 2). However, succinate transport activity in ISO vesicles expressing SdcS was inhibited after pretreatment with the MTS reagents; preincubation with MTSET decreased the rate of succinate uptake by ~85%, and preincubation with MTSES decreased the rate of uptake by ~90% (Figure 2). We also tested the membrane-permeant reagent MTSEA, which inhibited ISO vesicles completely but showed variable effects in RSO vesicles (results not shown). In two experiments, there was no effect of 1 mM MTSEA in RSO vesicles, and in two experiments, there was almost 100% inhibition. The membrane-permeant reagent, *N*-ethylmaleimide, inhibited SdcS in RSO vesicles by 73% (results not shown). RSO and ISO vesicles expressing the cysteine-less mutant, C457S, were insensitive to MTS reagents (results not shown), verifying that the single cysteine at position 457 in SdcS mediates the effects of these reagents. The results

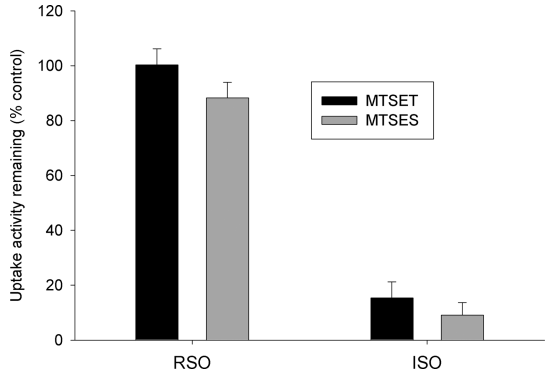

FIGURE 2: Effect of membrane-impermeant methanethiosulfonate (MTS) reagents on succinate uptake by SdcS in right-side-out (RSO) and inside-out (ISO) membrane vesicles. Vesicles were preincubated for 10 min with 1 mM methanethiosulfonate reagent (MTSET or MTSES) in buffer containing 5 mM Na^+ with or without MTS reagents (controls). The transport activity of 30 μM [^{14}C]succinate was measured in RSO and ISO vesicles with a 10 s incubation in buffer containing 10 mM Na^+. Uptake activities in vesicles preincubated with MTS reagents are expressed as a percentage of the uptake in control vesicles pretreated with Na^+ buffer alone. Bars represent the mean ± the range ($n = 2$ vesicle preparations).

show that the single cysteine at position 457 in SdcS is accessible to membrane-impermeant reagents only from the inside of the cell but not from the outside. In a single dose−response experiment, the $K_{0.5}$ for MTSET was 99 μM (result not shown).

It should be noted that membrane vesicle preparations often contain a mixture of orientations. For example, one study showed that RSO vesicle preparations from *E. coli* could contain between 5 and 25% ISO vesicles when counting numbers of vesicles (*17*). However, the ISO vesicles are much smaller in size and make up only 2−3% of the membrane surface area. Our time course experiment is consistent with this observation because the equilibrium vesicle volumes of ISO vesicles are smaller than those of RSO vesicles (Figure 1) The same study found that ISO membrane vesicles prepared using a French pressure cell were approximately 60−80% pure (*17*), although the sucrose density gradient step in our study might increase the purity of the ISO vesicles. One might expect to see some inhibition of "RSO membranes" by MTS reagents due to inhibition of contaminating ISO vesicles. It is possible that the smaller size and relatively lower transport activity of ISO vesicles could explain the lack of apparent inhibition.

Na^+ Activation of Succinate Transport in RSO and ISO Membrane Vesicles. SdcS is a sodium-coupled transporter. Therefore, the relationship between Na^+ concentration and succinate transport activity was examined in membrane vesicles expressing SdcS and C457S (Figure 3). Our previous transport studies of SdcS showed strong cation-mediated inhibition of succinate uptake at higher Na^+ concentrations in whole cell assays (*3*) but not in proteoliposomes (*18*). In preliminary studies with membrane vesicles, we found that succinate transport by SdcS expressed in RSO membrane vesicles was inhibited by sodium concentrations greater than 20 mM; therefore, the assay was done at lower sodium concentrations. The C457S mutant, in contrast, was not inhibited by sodium concentrations up to 80 mM (not shown). In the experiment shown in Figure 3A, activation of succinate transport by sodium was sigmoidal with Hill

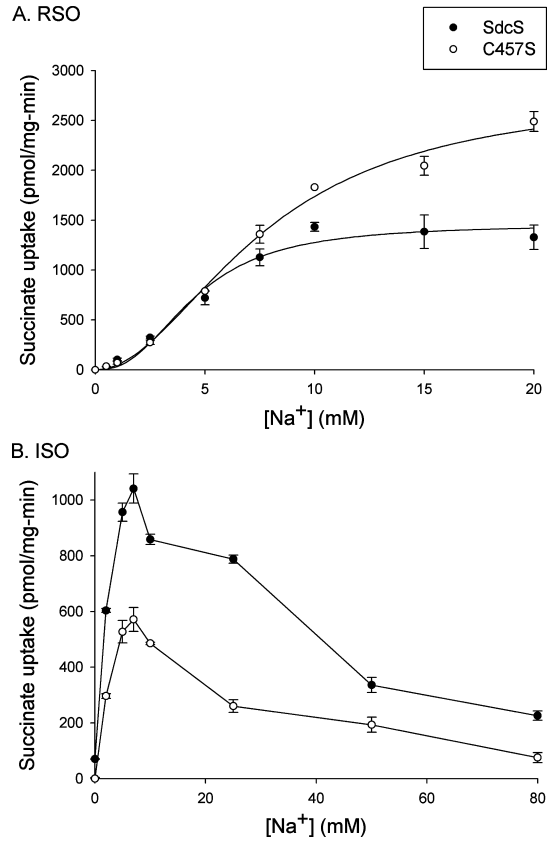

FIGURE 3: Effect of Na^+ on succinate uptake by SdcS and C457S. The transport of 30 μM [^{14}C]succinate was measured in (A) right-side-out and (B) inside-out vesicles for 10 s in an assay buffer containing 0−80 mM Na^+ (Na^+ was replaced by choline). The vesicles were prepared from *E. coli* expressing SdcS or C457S. Results are presented as means ± the range of duplicate measurements from a single vesicle preparation. The experiment was repeated with similar results with three separate vesicle preparations.

coefficients of 2.48 (SdcS) and 1.97 (C457S). The K_{Na} values for the experiment shown in Figure 3A were 4.5 mM (SdcS) and 7.7 mM (C457S). The average K_{Na} values in SdcS were 3.3 ± 0.6 mM ($n = 3$ experiments) and in C476S 8.2 ± 0.4 mM ($n = 5$ experiments), significantly different from one another at $p < 0.05$. In ISO vesicles, both SdcS and C457S were much more sensitive to inhibition by sodium, with decreased activity above 7 mM Na^+ and almost complete inhibition of activity at 80 mM Na^+ (Figure 3B).

Kinetics of Succinate Transport. Succinate kinetic analysis was performed for SdcS and C457S in RSO and ISO membrane vesicles. The K_m for succinate in SdcS was similar in RSO and ISO vesicles, 26 and 36 μM, respectively (Table 1). This value was higher than the previous K_m measurements of 7 μM in whole cells and 12 μM in proteoliposomes (*3, 18*). The V_{max} for succinate transport by SdcS in RSO vesicles was significantly higher than in ISO vesicles. The K_m values for succinate in C457S in RSO and ISO vesicles, 42 and 51 μM, respectively, were not significantly different from the values measured for SdcS. Similar to SdcS, C457S had a significantly higher succinate V_{max} in RSO compared with ISO vesicles. However, it should be noted that the volume differences between RSO and ISO vesicles could contribute to the apparent differences in V_{max} values.

Mutagenesis of SdcS. Previous studies with the rabbit NaDC1 have shown that cysteines substituted for residues Lys-

Table 1: Succinate Kinetics of SdcS and Mutants[a]

protein	orientation	K_m (μM)	V_{max} (pmol mg^{-1} min^{-1})	n
		Parental		
SdcS	RSO	26.4 ± 1.2	6742 ± 1456	3
	ISO	36.0 ± 4.3	2050 ± 303[b]	3
C457S	RSO	42.3 ± 8.0	5058 ± 509	3
	ISO	50.9 ± 7.5	1534 ± 118[b]	3
		Cysteine-Substituted Mutants		
N108C	RSO	46.6 ± 11.6	8115 ± 1292	3
	ISO	38.2 ± 7.2	2759 ± 1369[b]	3
D329C	RSO	44.5 ± 4.6	1069 ± 175[c]	3
	ISO	48.1 ± 2.5	1522 ± 192	3
L436C	RSO	149.2 ± 23.0[c]	3226 ± 362[c]	4
	ISO	36.1 ± 6.0[b]	2304 ± 921	4

[a] Succinate kinetics of SdcS and mutants in right-side-out (RSO) and inside-out (ISO) inner membrane vesicles from *E. coli*. Ten second uptakes were measured in transport buffer containing 10 mM Na^+ and increasing concentrations of [^{14}C]succinate. The data shown are means ± the standard error of the mean; n refers to the number of different vesicle preparations. [b] Significantly different from the RSO group ($p < 0.05$). [c] Significantly different from the C457S control group ($p < 0.05$).

```
                84              373             493
rbNaDC1   LEYLKDTNV       VMVSDGSAS       ILASMAQAI
SdcS      SEYGNDIIF       SSVADGTIA       ILATLSVAV
                108             329             436
```

FIGURE 4: Sequence alignment of SdcS with rabbit NaDC1. The sequence alignment was obtained using ClustalW2 (EMBL-EBI) with default parameters using the Gonnet matrix. Amino acids of SdcS in bold letters indicate amino acids that were substituted with cysteines. GenBank accession numbers of the protein sequences are AAA99666 (rbNaDC1) and BAB58078 (SdcS).

84, Asp-373, and Met-493 are accessible to membrane-impermeant methanethiosulfonate (MTS) reagents (*6, 7, 19*). D373C is accessible to MTSET in both the presence and absence of Na^+, and MTSET labeling is prevented by substrate. M493C and K84C require sodium for inhibition by MTS reagents, and they also show substrate protection. K84 is not sensitive to inhibition by MTSET, only by MTSES. These results show that the accessibility of these residues to the outside of the cell depends on the conformational state of the transporter. SdcS is approximately 40% identical in sequence to rbNaDC1, and Asn-108, Asp-329, and Leu-436 of SdcS correspond with Lys-84, Asp-373, and Met-493 of rbNaDC1, respectively (Figure 4). Therefore, the single cysteine-substituted mutants N108C, D329C, and L436C were constructed in the cysteine-less SdcS mutant, C457S. The accessibility of these substituted cysteines to MTS reagents from both sides of the membrane was then tested using RSO and ISO vesicles.

Protein Expression and Transport Activity of Cysteine-Substituted Mutants. The protein abundance of SdcS and mutants in RSO and ISO membrane vesicles was determined by Western blotting (Figures 5 and 6). The summary of succinate transport activity and protein expression of single-cysteine mutants is shown in Figure 6. In RSO vesicles, there was similar protein expression for SdcS, C457S, and the cysteine-substituted mutants. In SdcS, C457S, and L436C, the transport activity was similar to the relative amount of protein expression. However, N108C and D329C in RSO vesicles had much lower relative transport activity than protein expression. In the ISO vesicles, the level of protein expression of SdcS was about half that of the C457S mutant, whereas the transport activity of SdcS was higher than in C457S. The L436C mutant had lower activity compared with

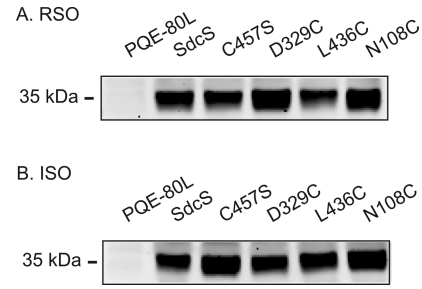

FIGURE 5: Western blots of membrane vesicles. Western blots were made of right-side-out (RSO) (A) and inside-out (ISO) membrane vesicles (B) expressing SdcS and cysteine-less C457S, N108C, D329C, and L436C. Control cells were transformed with the pQE-80L plasmid. Each lane contained 25 μg of protein. Proteins were detected using the RGS-His antibody (Qiagen), a monoclonal antibody against the N-terminal histidine tag. The mass of SdcS is approximately 35 kDa, indicated to the left of each blot.

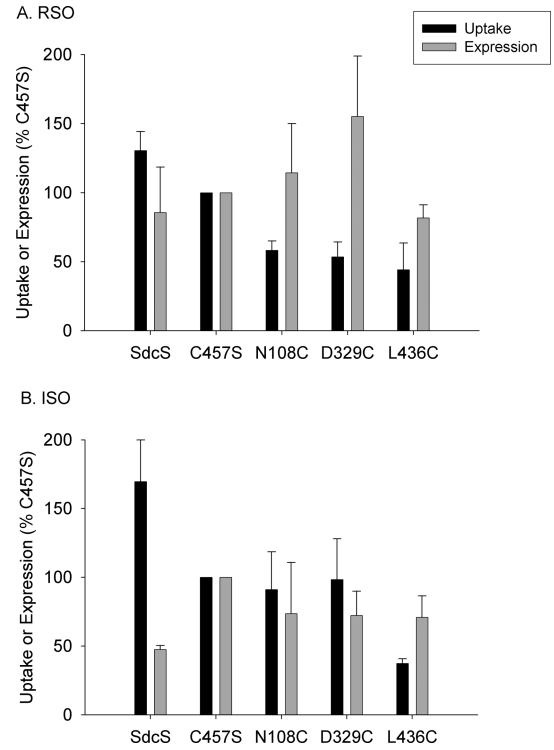

FIGURE 6: Comparison of activity and expression of (A) right-side-out and (B) inside-out membrane vesicles. The transport activity and protein abundance of membrane vesicles expressing the cysteine-substituted mutants are shown as a percentage of the C457S parental transporter. The transport activity of 30 μM [^{14}C]succinate was measured for 10 s in assay buffer containing 10 mM Na^+. Protein expression was determined by quantitating the intensities of SdcS vesicle protein bands from Western blots (such as in Figure 5) using Image 1D software. The bars represent means ± the standard error of the mean ($n = 3$ vesicle preparations).

protein expression, whereas the other mutants had similar relative activity and expression.

Succinate Kinetics in Cysteine-Substituted Mutants. The kinetics of succinate transport was measured in mutants N108C, D329C, and L436C in RSO and ISO membrane vesicles. As shown in Table 1, the K_m for succinate of mutant L436C in RSO vesicles was approximately 3.5-fold higher than that of the parental C457S. However, the K_m for succinate of the L436C mutant in ISO vesicles was similar to that of C457S. The other mutants had similar succinate affinity in RSO and ISO compared with C457S. The maximum velocities (V_{max}) of L436C and D329C mutants

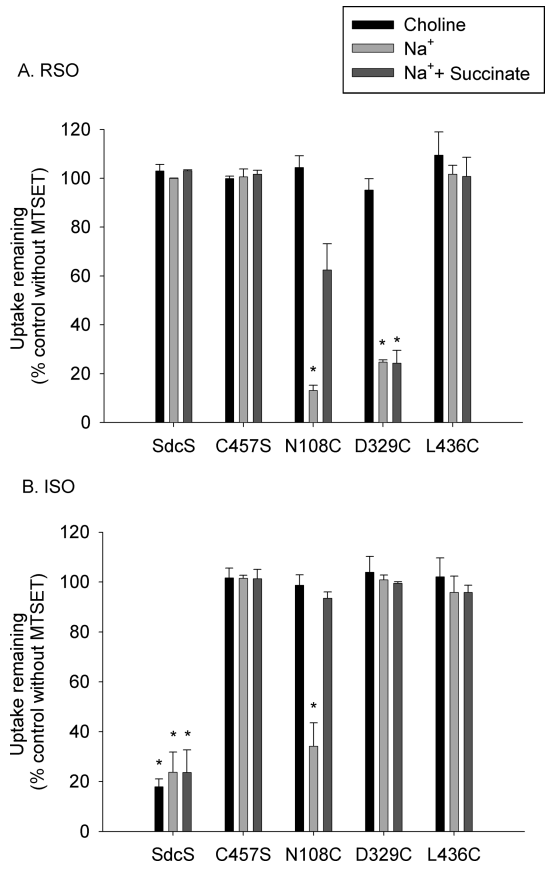

FIGURE 7: Effect of MTSET on succinate transport by cysteine-substituted SdcS mutants. (A) Right-side-out and (B) inside-out vesicles of cysteine-substituted mutants were preincubated for 10 min with 1 mM MTSET in buffers containing choline, Na^+, or Na^+ and 10 mM succinate. Control groups were preincubated in the same buffers without MTSET. Following the preincubation, the transport activity of 30 μM [^{14}C]succinate was measured for 10 s in a transport buffer containing 10 mM Na^+. Uptake activities in vesicles preincubated with MTSET are shown as a percentage of the uptakes in control vesicles. Bars represent means ± the standard error of the mean ($n = 3$ separate experiments). Asterisks indicate a significant difference compared with control (without MTSET) ($p < 0.05$).

in right-side-out vesicles were significantly lower than that of C457S. The cysteine-substituted mutants in ISO vesicles exhibited similar succinate K_m and V_{max} values as C457S.

MTSET Sensitivity of Cysteine-Substituted Mutants. To determine whether the substituted cysteines are accessible to MTSET in different conformational states of the transporter, the vesicles were pretreated with MTSET in different buffers: Na^+, choline (or Na^+-free), and 10 mM succinate in Na^+ buffer. Previous experiments suggest that SdcS follows an ordered binding mechanism in which Na^+ binds first followed by substrate (*3*). Therefore, different conformational states are likely to predominate in the presence and absence of Na^+ and substrate. SdcS in ISO vesicles was affected similarly by chemical labeling with MTSET in the presence or absence of Na^+ and substrate (Figure 7), indicating that the cysteine at position 457 is exposed to the cytoplasm in all conformational states. There was no effect of MTSET on SdcS in RSO vesicles or on the cysteine-less mutant, C457S, and L436C in RSO and ISO vesicles (Figure 7). Mutant N108C was accessible to MTSET in both RSO and ISO vesicles, and the inhibition by MTSET was greatest in the presence of sodium. There was substrate protection in both RSO and ISO vesicles containing N108C. Mutant D329C was only accessible to MTSET from the outside of the cell, in the RSO but not the ISO vesicles. MTSET labeling of D329C in RSO required sodium; there was no inhibition in choline buffer, and there was no substrate protection.

DISCUSSION

The kinetics and functional properties of the Na^+/dicarboxylate symporter SdcS from *S. aureus* were investigated by heterologous expression in *E. coli* followed by the preparation of right-side out (RSO) and inside out (ISO) membrane vesicles. The vesicles enabled us to examine the forward and reverse transport reactions as well as the accessibility of introduced cysteines from both sides of the membrane. Because SdcS is related in sequence to the mammalian Na^+/dicarboxylate cotransporters, studies of SdcS should provide information about the transport mechanism of other members of the SLC13 family. A major finding of this study was the identification of amino acid Asn-108 that is accessible from both the cytoplasmic and periplasmic sides of the membrane, indicating that it is found in the translocation pore of the protein.

Succinate transport by SdcS in both RSO and ISO vesicles exhibited an overshoot in concentration above equilibrium, verifying that it is an active transport process. The substrate affinity from the cytoplasmic and extracellular side appeared to be very similar with K_m values for succinate between 26 and 36 μM. However, the V_{max} of the forward reaction measured in RSO vesicles was higher than in ISO vesicles. It should be noted, though, that ISO vesicles tend to be much smaller than RSO vesicles (*17*), which could contribute to a lower V_{max}. Similar to SdcS, the rabbit Na^+/succinate cotransporter from renal brush-border membranes (most likely NaDC1) exhibits similar K_m values for influx and efflux but has a V_{max} for succinate influx 3 times higher than that for efflux (*20*). The succinate kinetic properties of the cysteine-less mutant, C457S, were very similar to those of wild-type SdcS.

The C457S mutant exhibited some differences from SdcS in sodium kinetics. Succinate transport by SdcS in RSO vesicles had a mean K_{Na} value of 3.3 mM and was inhibited by sodium concentrations above ~15 mM. In previous whole cell assays, the K_{Na} for sodium activation in SdcS was ~1.5 mM, and there was complete inhibition at high sodium concentrations (*3*). The cysteine-less mutant in RSO vesicles was relatively unaffected by high concentrations of sodium, with a higher mean K_{Na} of 8.2 mM, suggesting that Cys-457 may mediate the inhibition by sodium in particular conformational states of the transporter. In contrast, both the wild-type SdcS and C457S in ISO vesicles were inhibited by sodium concentrations above 7 mM. The transport inhibition at high sodium concentrations has also been reported for another bacterial transporter, Tyt1, assayed in whole cells (*21*). Interestingly, partially purified SdcS assayed in proteoliposomes no longer exhibits inhibition by high concentrations of sodium, which suggests that a protein in the *E. coli* membranes mediates the effect. One possible candidate could be the *E. coli* Na^+/H^+ exchanger, NhaA, which would transport Na^+ into the vesicle in exchange for protons. The activity of NhaA could result in succinate

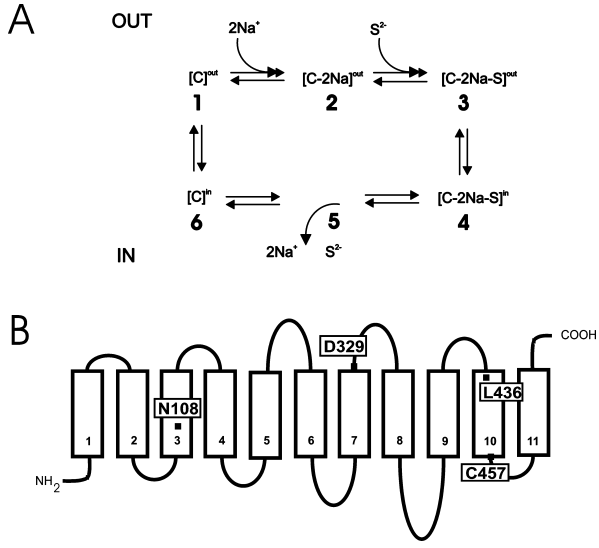

FIGURE 8: (A) Simplified kinetic model of SdcS. The transporter is shown as C with the substrate binding sites facing out of the cell (states 1−3) or facing inside the cell (states 4−6). There is ordered binding of two sodium ions followed by one divalent anion substrate (*3*). The fully loaded carrier undergoes a conformational change that exposes the substrate and cation binding sites to the inside of the cell. This is followed by release of substrate and sodium, in an as yet unknown order. The empty carrier then reorients the substrate and cation binding sites to face the outside. (B) Secondary structure model of SdcS containing 11 transmembrane helices (numbered) with an intracellular amino terminus and extracellular carboxy terminus. The locations of the single cysteine at position 457 and the three cysteine-substituted mutants, N108C, D329C, and L436C, are shown as filled black squares.

transport inhibition by collapsing the Na^+ gradient, *trans*-inhibition with an increased intracellular Na^+ concentration, or inhibition due to a change in intravesicular pH. SdcS has a pH optimum of approximately 7−7.4, and alkalinization would result in decreased activity (*3*). It is possible that the effects are more pronounced in ISO because of their smaller size.

The transport mechanism of SdcS involves ordered binding of two sodium ions followed by binding of substrate (*3*). A simplified kinetic model with six states is shown in Figure 8A. The results of this study show that residue Asn-108 from SdcS is accessible from the extracellular as well as the cytoplasmic side of the cell. Asn-108 of SdcS corresponds to Lys-84 of rbNaDC1, which has different accessibility to the outside of the cell during the transport cycle, and it is likely located within the substrate binding pocket (*7, 22*). The N108C mutant of SdcS was sensitive to inhibition by MTSET in the conformation adopted in the presence of Na^+. In RSO vesicles in Na^+ buffer, SdcS should be predominantly in state 2, an outward-facing conformation with Na^+ ions bound to the transporter (Figure 8A). This state has the highest affinity for substrate. In ISO vesicles in the presence of sodium, the transporter should be predominantly state 5, the Na^+-bound conformation facing the cytoplasmic side of the membrane (Figure 8A). Note that the cytoplasmic side of the membrane faces out in inverted vesicles.

The N108C mutant also exhibited substrate protection of MTSET labeling, which was due to steric hindrance rather than a conformational change in the protein. Because the mutation of Asn-108 did not change the kinetic properties of the transporter, it is likely that this residue is located near the substrate binding site but is not part of it. Figure 8B shows the secondary structure model of SdcS, based on the rbNaDC1 model, with Asn-108 located approximately midway through TM3. Asn-108 could be exposed alternately to the inside and outside of the cell by tilting or twisting of TM3. Similar results were seen previously for the UhpT transporter in which cysteine mutants located in the central portion of transmembrane helix 7 are accessible to both the outside and inside of the cell (*23, 24*). These residues also exhibited substrate protection (*24*). The endogenous cysteine at position 176 in TM5 of the glycerol 3-phosphate transporter, GlpT, is also located in the transport pathway (*25*). Cys-176 is accessible to pCMBS from both the outside and inside of the cell, and the accessibility is blocked by the presence of substrate. However, an alternate explanation for our results is that Asn-108 of SdcS resides in a re-entrant loop that changes accessibility during the transport cycle. The Na^+-citrate symporter CitS contains two endogenous cysteines, accessible from both sides of the membrane, that are found in a re-entrant loop lining part of the substrate permeability pathway (*26*).

Mutant D329C of SdcS was accessible to MTSET in the presence but not absence of Na^+ and only in RSO vesicles, indicating that its accessibility also changes in the different conformational states of the transporter. The accessibility of D329C would be greatest in states 2 and 3 (Figure 8). This aspartic acid residue is conserved among all members of the SLC13 family. The secondary structure model places this residue at the extracellular surface of TM7, explaining its accessibility from the outside (Figure 10). The L436C mutant of SdcS was not affected by MTSET, which could mean that Leu-436 is buried in the helix and not accessible to the outside or that chemical labeling by MTSET does not have any functional effect. This residue appears to determine substrate affinity in the forward direction (from outside to inside) because L436C in RSO membrane vesicles showed a 3.5-fold higher K_m compared with that for ISO vesicles. The other members of the SLC13 family contain either leucine or methionine in this position. By comparison, the M493C mutant (at the equivalent position) of rbNaDC1 is very sensitive to inhibition by MTSET (*6*).

The results of this study, particularly with the N108C mutant, are consistent with the alternating access model of transport in which the transporter protein contains a single substrate binding site that is alternately accessible from both sides of the membrane. The lactose permease (LacY) and glycerol-3-phosphate transporter (GlpT), both secondary active transporters from the major facilitator superfamily, follow an alternating access mechanism for transport of substrates (*23, 27−29*). The structure of the lactose permease shows a large water-filled cavity containing the amino acid side chains involved in binding protons and substrate (*27*). Experiments involving cross-linking of residues in LacY show that transport activity involves opening and closing of the hydrophilic cavity (*30*). The structure of GlpT has a funnel-shaped vestibule leading to the substrate binding site (*31*). Similar to LacY, the GlpT structure suggests a rocker-switch-type movement of two halves of the protein during the transport cycle, involving salt bridge formation and breakage.

This work represents the characterization of SdcS in RSO and ISO membrane vesicles. The kinetic properties of

succinate transport in SdcS appear asymmetrical, which may indicate differences in transport velocity (V_{max}) rather than substrate affinity. The N108C mutant of SdcS was found to be accessible to membrane-impermeant methanethiosulfonate reagents from both sides of the membrane, indicating that this residue may be located within the translocation pathway of the transporter, possibly close to the substrate binding site. The sensitivity of mutant D329C to MTSET inhibition was greatest in RSO vesicles in the presence of sodium, whereas residue Leu-436 may be a determinant of substrate affinity in the forward direction, measured in RSO vesicles. In conclusion, this study establishes SdcS as a model system for the eukaryotic NaDC1 transporters and identifies key residues, particularly Asn-108, that may be important during the transport cycle from both sides of the membrane.

ACKNOWLEDGMENT

We thank Dr. Matthias Quick for the use of his membrane vesicle protocols and discussions about *E. coli* membrane preparations. Thanks also to Kathleen Randolph for preparation of bacterial media and solutions.

REFERENCES

1. Prakash, S., Cooper, G., Singhi, S., and Saier, M. H., Jr. (2003) The ion transporter superfamily. *Biochim. Biophys. Acta 1618*, 79–92.
2. Pajor, A. M. (2006) Molecular properties of the SLC13 family of dicarboxylate and sulfate transporters. *Pfluegers Arch. 451*, 597–605.
3. Hall, J. A., and Pajor, A. M. (2005) Functional characterization of a Na^+-coupled dicarboxylate carrier protein from *Staphylococcus aureus*. *J. Bacteriol. 187*, 5189–5194.
4. Oshiro, N., King, S. C., and Pajor, A. M. (2006) Transmembrane helices 3 and 4 are involved in substrate recognition by the Na^+/dicarboxylate cotransporter, NaDC1. *Biochemistry 45*, 2302–2310.
5. Pajor, A. M. (2001) Conformationally sensitive residues in transmembrane domain 9 of the Na^+/dicarboxylate cotransporter. *J. Biol. Chem. 276*, 29961–29968.
6. Pajor, A. M., and Randolph, K. M. (2005) Conformationally sensitive residues in extracellular loop 5 of the Na^+/dicarboxylate co-transporter. *J. Biol. Chem. 280*, 18728–18735.
7. Weerachayaphorn, J., and Pajor, A. M. (2007) Sodium-dependent extracellular accessibility of Lys-84 in the sodium/dicarboxylate cotransporter. *J. Biol. Chem. 282*, 20213–20220.
8. Yamashita, A., Singh, S. K., Kawate, T., Jin, Y., and Gouaux, E. (2005) Crystal structure of a bacterial homologue of Na^+/Cl^- dependent neurotransmitter transporters. *Nature 437*, 215–223.
9. Yernool, D., Boudker, O., Jin, Y., and Gouaux, E. (2004) Structure of a glutamate transporter homologue from *Pyrococcus horikoshii*. *Nature 431*, 811–818.
10. Kaback, H. R. (1971) Bacterial membranes. *Methods Enzymol. 22*, 99–120.
11. Lolkema, J. S., Enequist, H., and van der Rest, M. E. (1994) Transport of citrate catalyzed by the sodium-dependent citrate carrier of *Klebsiella pneumoniae* is obligatorily coupled to the transport of two sodium ions. *Eur. J. Biochem. 220*, 469–475.
12. Quick, M., and Jung, H. (1998) A conserved aspartate residue, Asp187, is important for Na^+-dependent proline binding and transport by the Na^+/proline transporter of *Escherichia coli*. *Biochemistry 37*, 13800–13806.
13. Quick, M., Tomasevic, J., and Wright, E. M. (2003) Functional asymmetry of the human Na^+/glucose transporter (hSGLT1) in bacterial membrane vesicles. *Biochemistry 42*, 9147–9152.
14. Schnaitman, C. A. (1970) Protein composition of the cell wall and cytoplasmic membrane of *Escherichia coli*. *J. Bacteriol. 104*, 890–901.
15. Wright, S. H., Hirayama, B., Kaunitz, J. D., Kippen, I., and Wright, E. M. (1983) Kinetics of sodium succinate cotransport across renal brush-border membranes. *J. Biol. Chem. 258*, 5456–5462.
16. Pajor, A. M., Sun, N., and Valmonte, H. G. (1998) Mutational analysis of histidines in the Na^+/dicarboxylate cotransporter, NaDC1. *Biochem. J. 331*, 257–264.
17. Altendorf, K. H., and Staehelin, L. A. (1974) Orientation of membrane vesicles from *Escherichia coli* as detected by freeze-cleave electron microscopy. *J. Bacteriol. 117*, 888–899.
18. Hall, J. A., and Pajor, A. M. (2007) Functional reconstitution of SdcS, a Na^+-coupled dicarboxylate carrier protein from *Staphylococcus aureus*. *J. Bacteriol. 189*, 880–885.
19. Yao, X., and Pajor, A. M. (2002) Arginine-349 and aspartate-373 of the Na^+/dicarboxylate cotransporter are conformationally sensitive residues. *Biochemistry 41*, 1083–1090.
20. Hirayama, B., and Wright, E. M. (1984) Asymmetry of the Na^+-succinate cotransporter in rabbit renal brush-border membranes. *Biochim. Biophys. Acta 775*, 17–21.
21. Quick, M., Yano, H., Goldberg, N. R., Duan, L., Beuming, T., Shi, L., Weinstein, H., and Javitch, J. A. (2006) State-dependent conformations of the translocation pathway in the tyrosine transporter Tyt1, a novel neurotransmitter:sodium symporter from *Fusobacterium nucleatum*. *J. Biol. Chem. 281*, 26444–26454.
22. Pajor, A. M., Kahn, E. S., and Gangula, R. (2000) Role of cationic amino acids in the sodium/dicarboxylate co-transporter NaDC-1. *Biochem. J. 350*, 677–683.
23. Huang, Y., Lemieux, M. J., Song, J., Auer, M., and Wang, D. N. (2003) Structure and mechanism of the glycerol-3-phosphate transporter from *Escherichia coli*. *Science 301*, 616–620.
24. Yan, R. T., and Maloney, P. C. (1995) Residues in the pathway through a membrane transporter. *Proc. Natl. Acad. Sci. U.S.A. 92*, 5973–5976.
25. Fann, M. C., Busch, A., and Maloney, P. C. (2003) Functional characterization of cysteine residues in GlpT, the glycerol 3-phosphate transporter of *Escherichia coli*. *J. Bacteriol. 185*, 3863–3870.
26. Sobczak, I., and Lolkema, J. S. (2004) Alternating access and a pore-loop structure in the Na^+-citrate transporter CitS of *Klebsiella pneumoniae*. *J. Biol. Chem. 279*, 31113–31120.
27. Abramson, J., Smirnova, I., Kasho, V., Verner, G., Kaback, H. R., and Iwata, S. (2003) Structure and mechanism of the lactose permease of *Escherichia coli*. *Science 301*, 610–615.
28. Kaback, H. R., Dunten, R., Frillingos, S., Venkatesan, P., Kwaw, I., Zhang, W., and Ermolova, N. (2007) Site-directed alkylation and the alternating access model for LacY. *Proc. Natl. Acad. Sci. U.S.A. 104*, 491–494.
29. Lemieux, M. J., Huang, Y., and Wang, D. N. (2004) The structural basis of substrate translocation by the *Escherichia coli* glycerol-3-phosphate transporter: A member of the major facilitator superfamily. *Curr. Opin. Struct. Biol. 14*, 405–412.
30. Zhou, Y., Guan, L., Freites, J. A., and Kaback, H. R. (2008) Opening and closing of the periplasmic gate in lactose permease. *Proc. Natl. Acad. Sci. U.S.A. 105*, 3774–3778.
31. Law, C. J., Maloney, P. C., and Wang, D. N. (2008) Ins and outs of major facilitator superfamily antiporters. *Annu. Rev. Microbiol. 62*, 289–305.

BI8022625